

$B \rightarrow D_0^*$ and $B_s \rightarrow D_{s0}^*$ form factors from QCD light-cone sum rules

Nico Gubernari^{a*}, Alexander Khodjamirian^{a†}, Rusa Mandal^{b‡}, and Thomas Mannel^{a§}

^a*Center for Particle Physics Siegen (CPPS), Theoretische Physik 1,
Universität Siegen, 57068 Siegen, Germany*

^b*Indian Institute of Technology Gandhinagar, Department of Physics,
Gujarat 382355, India*

Abstract

We present the first application of QCD light-cone sum rules (LCSRs) with $B_{(s)}$ -meson distribution amplitudes to the $B_{(s)} \rightarrow D_{(s)0}^*$ form factors, where $D_{(s)0}^*$ is a charmed scalar meson. We consider two scenarios for the D_0^* spectrum. In the first one, we follow the Particle Data Group and consider a single broad resonance $D_0^*(2300)$. In the second one, we assume the existence of two scalar resonances, $D_0^*(2105)$ and $D_0^*(2451)$, as follows from a recent theoretically motivated analysis of $B \rightarrow D\pi\pi$ decays. The $B \rightarrow D_0^*$ form factors are calculated in both scenarios, also taking into account the large total width of $D_0^*(2300)$. Furthermore, we calculate the $B_s \rightarrow D_{s0}^*$ form factors, considering in this case only the one-resonance scenario with $D_{s0}^*(2317)$. In this LCSR calculation, the c -quark mass is kept finite and the s -quark mass is taken into account. We also include contributions of the two- and three-particle distribution amplitudes up to twist-four. Our predictions for semileptonic $B \rightarrow D_0^*\ell\nu_\ell$ and $B_s \rightarrow D_{s0}^*\ell\nu_\ell$ branching ratios are compared with the available data and HQET-based predictions. As a byproduct, we also obtain the D_0^* - and D_{s0}^* -meson decay constants and predict the lepton flavour universality ratios $R(D_0^*)$ and $R(D_{s0}^*)$.

*Email: nico.gubernari@gmail.com

†Email: khodjamirian@physik.uni-siegen.de

‡Email: rusa.mandal@iitgn.ac.in

§Email: mannel@physik.uni-siegen.de

Contents

1	Introduction	2
2	Charmed scalar mesons	3
3	Two-point QCD sum rules for charmed scalar mesons	4
3.1	Hadronic representations of the two-point correlator	5
3.2	OPE of the two-point correlators	7
3.3	Sum rules and numerical results for decay constants	8
4	LCSRs for the $B_{(s)} \rightarrow D_{(s)0}^*$ form factors	10
4.1	Hadronic dispersion relation	11
4.2	Light-cone OPE for the correlator	13
4.3	Light-cone sum rules and numerical results for the form factors	15
5	Conclusion	21
A	Light-Cone DAs of B-meson	22
B	OPE coefficients	24
B.1	Contributions of two-particle DAs	24
B.2	Contributions of three-particle DAs	25

1 Introduction

The semileptonic $b \rightarrow c\ell\bar{\nu}_\ell$ transitions are predominantly realised in the form of exclusive $\bar{B} \rightarrow D\ell\bar{\nu}_\ell$ and $\bar{B} \rightarrow D^*\ell\bar{\nu}_\ell$ decays and their \bar{B}_s counterparts. No less important but considerably less studied are the subdominant exclusive decays $\bar{B} \rightarrow D_J^*\ell\bar{\nu}_\ell$ and $\bar{B}_s \rightarrow D_{sJ}^*\ell\bar{\nu}_\ell$, where D_J^* and D_{sJ}^* are excited charmed mesons with spin-parity $J^P = 0^+, 1^+, 2^+$. Apart from filling the gap between the inclusive $\bar{B} \rightarrow X_c\ell\bar{\nu}_\ell$ width and the sum over partial widths of exclusive channels, these decays are important also for deciphering the spectroscopy of excited charmed mesons which is still far from being firmly established. Indeed, currently, the main information on the masses and widths of D_J^* mesons stems from the analyses of the nonleptonic three-body B -decays in which one has to disentangle complicated final-state interactions. Semileptonic decays such as $\bar{B} \rightarrow D^{(*)}\pi\ell\bar{\nu}_\ell$ are in this respect much simpler for an extraction of D_J^* resonances in the $D^{(*)}\pi$ states. It is also possible to use the $\bar{B} \rightarrow D_J^*\ell\bar{\nu}_\ell$ decays as an alternative channel to probe the $b \rightarrow c\ell\bar{\nu}_\ell$ transitions for the presence of New Physics. To this end, however, one would need more precise experimental measurements and theoretical predictions. In addition, these decay channels are important because they constitute one of the main backgrounds in the $\bar{B} \rightarrow D^*\ell\bar{\nu}_\ell$ measurements.

The key element needed to obtain predictions for any exclusive semileptonic decay is a set of process-dependent hadronic form factors. The lattice QCD methods, well advanced in calculating the $B \rightarrow D$ and $B \rightarrow D^*$ form factors, are not yet able to describe the B -meson transitions to unstable charmed mesons, especially to the broad resonant $D^{(*)}\pi$ states with $J^P = 0^+, 1^+$. In our previous paper [1], we obtained the form factors of the B -meson transitions to the charmed

axial mesons with $J^P = 1^+$, applying the QCD light-cone sum rules (LCSRs) with B -meson distribution amplitudes (DAs). This version of the LCSR method is very versatile, as it allows the spin parity and flavour of the final hadronic state to be varied by adjusting the interpolating quark-antiquark current in the underlying correlation function.

In this paper we use LCSRs with B -meson DAs to calculate for the first time the $B \rightarrow D_0^*$ and $B_s \rightarrow D_{s0}^*$ form factors, including the contributions of three-particle B -meson DAs up to twist-four.¹ Important additional elements of this paper are also the two-point QCD sum rules for the decay constants of D_0^* . The correlation functions used here and in Ref. [1] are very similar, up to a replacement of the charmed-meson interpolating current.

In the case of charmed axial mesons, there was a problem to separate the form factors for two very close D_1^* resonances. The solution found in Ref. [1] was to introduce a second interpolating current and to use linear combinations of LCSRs and of two-point sum rules with two different currents. In the case of charmed scalar mesons the hadronic parts of the sum rules do not pose such a problem. Instead, we are faced with two alternatives concerning the experimentally observed charmed scalar mesons. According to Ref. [4], the lightest meson is identified with the broad $D_0^*(2300)$ resonance decaying into $D\pi$ in the S wave. On the other hand, in recent theory-based analysis of $B \rightarrow D\pi\pi$ decays (see Refs. [5,6] and references therein) a different configuration of charmed scalar mesons was found, consisting of the two well separated resonances, $D_0^*(2105)$ and $D_0^*(2451)$. In particular, the lowest state $D_0^*(2105)$ is interpreted as a product of nonperturbative dynamics of the low-energy pion scattering off D -meson, analogous to the lightest scalar nonstrange and strange mesons, $f_0(600)$ and $K_0^*(700)$. The latter are usually interpreted (see, e.g. the review on scalar mesons in Ref. [4]) as molecular and/or tetraquark objects rather than quark-antiquark states. The existence of a lighter charmed scalar meson than the one identified in Ref. [4] was also supported by a recent lattice QCD computation [7] of the isospin $1/2$ $D\pi$ scattering amplitudes.

We will consider both the one-resonance and the two-resonance scenarios for the charmed scalar mesons and compute the respective decay constants and form factors. For the charmed-strange scalar meson we limit ourselves to the single resonance scenario, since the ground state is narrow and well established experimentally.

The plan of this paper is as follows. In Section 2, we introduce and discuss both scenarios of the spectrum of charmed and charmed-strange scalar mesons. In Section 3, we use the two-point QCD sum rules to obtain the decay constants of these mesons. Section 4 is devoted to the LCSRs for the form factors and their numerical analysis, including the prediction of selected physical observables. Finally, section 5 contains the concluding discussion. The paper has two appendices: in A we collect the definitions and the models for the B -meson light-cone DAs and in B we present the expressions for the OPE coefficients of our LCSRs.

2 Charmed scalar mesons

For the QCD sum rules and LCSRs to be obtained below we need as an input the masses and the widths of the lowest charmed and charmed-strange scalar mesons. Here we discuss the two alternatives already mentioned in the Introduction. As a default choice (scenario 1), we adopt the

¹Earlier, the three-point QCD sum rules based on the local OPE and double dispersion relation have been used for the $B \rightarrow D_0^*$ form factors in Ref. [2] (see also the HQET analogue of these sum rules in Ref. [3]).

Scenario	Meson	Mass [MeV]	Width [MeV]
1	$D_0^* \equiv D_0^*(2300)$	2343 ± 10	229 ± 16
	$D_{s0}^* \equiv D_{s0}^*(2317)$	2317.8 ± 0.5	< 3.8
2	$D_0^* \equiv D_0^*(2105)$	2105_{-6}^{-8}	204_{-22}^{+20}
	$D_0^{*'} \equiv D_0^*(2451)$	2451_{+35}^{-26}	268_{-16}^{+14}
	$D_{s0}^* \equiv D_{s0}^*(2317)$	2317.8 ± 0.5	< 3.8
	$D_{s0}^{*'} \equiv D_{s0}^*(2660)$	~ 2660	—

Table 1: *The lowest-lying charmed scalar ($J^P = 0^+$) mesons. For scenario 1 (scenario 2) we take the masses and total widths from Ref. [4] (from Refs. [5, 6]), except the mass of $D_{s0}^{*'}$ which is our estimate.*

single resonance $D_0^*(2300)$ as it is currently listed in Ref. [4]. A rather strong argument against this choice is that in this case the corresponding charmed-strange meson $D_{s0}^*(2317)$ seems to be unnaturally light. Indeed, the mass difference between strange and nonstrange resonances does not fit the expected order of m_s . Note that, according to Ref. [4], the mass and width of the $D_0^*(2300)$ resonance is obtained from Dalitz-plot analysis of the weak $B \rightarrow D\pi\pi$ decays. The mass of its strange counterpart $D_{s0}^*(2317)$ is, on the contrary, more directly determined from the $e^+e^- \rightarrow D_{s0}^* \bar{D}_s$ cross section with the subsequent $D_{s0}^* \rightarrow D_s \pi^0$ decay [8].

The second alternative for charmed scalar mesons is markedly different and originates from the analysis done in Refs. [5, 6], and in earlier papers cited therein. Here, again the data on $B \rightarrow D\pi\pi$ decay are used, more specifically, the most accurate recent measurements by LHCb [9]. Without going into details which are beyond the scope of this paper, we only mention that in this analysis the S -wave $D\pi$ scattering amplitude is isolated in the final-state interaction of the $B \rightarrow D\pi\pi$ decay and the resonance structure of this amplitude is extracted. The outcome is a prediction of two resonances $D_0^*(2105)$ and $D_0^*(2451)$ replacing the single one suggested in Ref. [4]. The first of these resonances solves the above mentioned problem of the mass difference between strange and nonstrange states. Simultaneously, the second one indicates the existence of a second charmed-strange state, the analog of $D_0^*(2451)$. Adding to its mass the difference between the $D_{s0}^*(2317)$ and $D_0^*(2105)$ masses, we roughly locate this state at around 2660 MeV.

It is very important to reestablish or test these predictions in a more clean hadronic environment provided by semileptonic decay $B \rightarrow D\pi\ell\nu$. To this end, one needs an accurate partial wave reconstruction of the $D\pi$ state, an isolation of the S -wave component and a study of its resonance structure. Needless to say, a theory prediction for the underlying $B \rightarrow D_0^*$ transition form factors is important for such an analysis.

3 Two-point QCD sum rules for charmed scalar mesons

The decay constants of the charmed scalar meson and its charmed-strange counterpart are essential inputs for the LCSRs for the $B_{(s)} \rightarrow D_{(s)0}^*$ form factors. Since there is no available

estimate of these quantities and in particular no lattice QCD computation, we calculate them using QCD sum rules. We derive these sum rules starting from the two-point correlators

$$\Pi^{(s)}(q^2) = i \int d^4x e^{iqx} \langle 0 | \mathcal{T} \{ J_{(s)}(x) J_{(s)}^\dagger(0) \} | 0 \rangle, \quad (3.1)$$

where

$$J = (m_c - m_d) \bar{c}d \quad \text{and} \quad J_s = (m_c - m_s) \bar{c}s \quad (3.2)$$

are the interpolating quark currents for the D_0^* and D_{s0}^* meson, respectively. The currents in Eq. (3.2) coincide with the divergences of the corresponding vector currents. These currents have no anomalous dimension. We assume isospin symmetry and chiral limit for the u, d quarks in the correlators, so that the sum rules for the charged and neutral D_0^* mesons coincide. We however retain the s -quark mass throughout our computations, hence the violation of $SU(3)_{fl}$ symmetry is to a large extent taken into account.

In the remainder of this section, we derive the two-point QCD sum rules for the decay constants $f_{D_0^{*(\prime)}}$ and $f_{D_{s0}^*}$, which are defined as

$$\langle 0 | J | D_0^{*(\prime)}(p) \rangle = m_{D_0^{*(\prime)}}^2 f_{D_0^{*(\prime)}}, \quad \langle 0 | J_s | D_{s0}^*(p) \rangle = m_{D_{s0}^*}^2 f_{D_{s0}^*}. \quad (3.3)$$

In Subsection 3.1, following the scenarios outlined in Table 1, we consider two different hadronic representations of the correlators (3.1), while in Subsection 3.2 we calculate the same correlators using an OPE. Following the usual procedure to derive a QCD sum rule, in Subsection 3.3 we match the hadronic representations with the corresponding OPE expressions and use the quark-hadron duality approximation. We also perform a numerical analysis of the resulting sum rules and obtain the values of the decay constants.

3.1 Hadronic representations of the two-point correlator

Following the two scenarios for the spectrum of the lowest-lying charmed scalar mesons discussed in Section 2 and specified in Table 1, we consider two different hadronic representation of the correlator (3.1).

Scenario 1

In this case there is only one resonance, i.e. D_0^* , and hence the two-point QCD sum rule is derived using the standard procedure of Ref. [10]. The hadronic dispersion relation for the correlator (3.1) can be written as

$$\Pi_{\text{had}}(q^2) = \int_0^\infty ds \frac{\rho_{\text{had}}(s)}{s - q^2}, \quad (3.4)$$

where subtractions are not shown for simplicity and the hadronic spectral density ρ_{had} is given by

$$\rho_{\text{had}}(s) = f_{D_0^*}^2 m_{D_0^*}^4 \delta(m_{D_0^*}^2 - s) + \rho_{\text{cont}}(s) \theta(s - s_{\text{th}}). \quad (3.5)$$

Here, ρ_{cont} is the spectral density of continuum and excited states without the contribution of the D_0^* resonance and $s_{\text{th}} = (m_D + m_\pi)^2$ is the lowest continuum threshold. The scalar resonances are always located above this threshold and hence there is no gap between them and the continuum hadronic states in this channel. The situation resembles the light-quark vector and scalar channels where the corresponding resonances (ρ and f_0 , respectively) are also located above the two-pion threshold. Since here, similar to the conventional QCD sum rules for light mesons, we will apply the quark-hadron duality and replace the integral over $\rho_{\text{cont}}(s)$ by the integrated OPE density, the detailed structure of ρ_{cont} plays no role.

We then substitute the spectral density (3.5) into the dispersion relation and perform a Borel transform with respect to the variable q^2 to remove the subtraction terms and to exponentially suppress the contribution of ρ_{cont} :

$$\Pi_{\text{had}}(M^2) = f_{D_0^*}^2 m_{D_0^*}^4 e^{-m_{D_0^*}^2/M^2} + \int_{s_{\text{th}}}^{\infty} ds \rho_{\text{cont}}(s) e^{-s/M^2}. \quad (3.6)$$

The hadronic representation for the correlator Π^s can be obtained from the above equation with obvious replacements and taking into account that $s_{\text{th}} = (m_D + m_K)^2$ in this case. Note that a lighter $D_s\pi$ state is decoupled in the isospin symmetry limit.

Furthermore, we take into account the large total width of the D_0^* meson by replacing

$$e^{-m_{D_0^*}^2/M^2} \rightarrow \mathcal{E}(\Gamma_{D_0^*}, M^2) \equiv \int_{s_{\text{th}}}^{\infty} ds e^{-s/M^2} \left[\frac{1}{\pi} \frac{\sqrt{s} \Gamma_{D_0^*}(s)}{(s - m_{D_0^*}^2)^2 + s \Gamma_{D_0^*}^2(s)} \right]. \quad (3.7)$$

The energy-dependent width $\Gamma_{D_0^*}(s)$ is defined in terms of the total width of D_0^* , assuming that the two-particle $D\pi$ state is the dominant final state, hence taking the S -wave phase-space factor

$$\Gamma_{D_0^*}(s) = \Gamma_{D_0^*}^{\text{tot}} \left[\frac{\lambda^{1/2}(s, m_D^2, m_\pi^2) m_{D_0^*}}{\lambda^{1/2}(m_{D_0^*}^2, m_D^2, m_\pi^2) \sqrt{s}} \right], \quad (3.8)$$

where λ is the Källén function and $\Gamma_{D_0^*}^{\text{tot}}$ is the total width. In the narrow-width limit, i.e. for $\Gamma_{D_0^*}^{\text{tot}} \rightarrow 0$, the expression inside square brackets in Eq. (3.7) becomes a δ -function and $\mathcal{E}(\Gamma_{D_0^*}, M^2) = e^{-m_{D_0^*}^2/M^2}$ is restored. For the strange D_{s0}^* meson, it is sufficient to consider only the narrow resonance approximation, since its measured total width is very small.

Scenario 2

In this case, we need to disentangle the two resonances, i.e. D_0^* and $D_0'^*$, to obtain the respective decay constants separately. The sum rule for the lighter charmed meson D_0^* is again derived using the standard procedure. Here, one benefits from the fact that the second resonance $D_0'^*$ is about 350 MeV heavier. Thus, a duality interval can be reliably determined, so that the heavier resonance is considered a part of the spectral density ρ_{cont} . This yields again Eqs. (3.4)-(3.5), but with a different numerical value of $m_{D_0^*}$ (as given in Table 1) and, correspondingly, with a different spectral density ρ_{cont} .

To derive the sum rule for $D_0^{*'}$ we start from the hadronic dispersion relation with isolated contributions of two resonances. After performing the Borel transform we have

$$\Pi_{\text{had}}(M^2) = f_{D_0^*}^2 m_{D_0^*}^4 e^{-m_{D_0^*}^2/M^2} + f_{D_0^{*'}}^2 m_{D_0^{*'}}^4 e^{-m_{D_0^{*'}}^2/M^2} + \int_{s_{\text{th}}}^{\infty} ds \tilde{\rho}_{\text{cont}}(s) e^{-s/M^2}, \quad (3.9)$$

where $\tilde{\rho}_{\text{cont}}(s)$ is now defined as the spectral density of continuum and excited states without the contributions of the two lower resonances.

We then follow Ref. [11], where the sum rules for radially excited heavy-light mesons were obtained, and eliminate the contribution of the lighter resonance in the above relation by applying the operator

$$\mathcal{D} \equiv \frac{d}{d(1/M^2)} + m_{D_0^*}^2 \quad (3.10)$$

which yields

$$\mathcal{D}\Pi_{\text{had}}(M^2) = f_{D_0^{*'}}^2 (m_{D_0^*}^2 - m_{D_0^{*'}}^2) m_{D_0^{*'}}^4 e^{-m_{D_0^{*'}}^2/M^2} + \int_{s_{\text{th}}}^{\infty} ds (m_{D_0^*}^2 - s) \tilde{\rho}_{\text{cont}}(s) e^{-s/M^2}. \quad (3.11)$$

This procedure enables us to derive the sum rule for the decay constant of the second resonance. In this scenario, we neglect the meson widths for simplicity. For charmed-strange mesons, we postpone the two-resonance scenario, until there is evidence for the second charmed-strange scalar resonance.

3.2 OPE of the two-point correlators

In the spacelike region, $q^2 \ll m_c^2$, we calculate the correlator (3.1), applying the OPE in local operators. The result can be written as a truncated series of vacuum averaged operators of increasing dimension d . Their corresponding Wilson coefficients depend on the choice of interpolating currents and encode the short-distance propagation of virtual quarks in the correlator. The leading power contribution is given by the $d = 0$ unit operator multiplied by the corresponding Wilson coefficient and represents a purely perturbative contribution to the correlator (3.1). The contributions of higher dimensional operators, starting from $d = 3$, are reduced to vacuum condensates which encode the non-perturbative QCD effects in a universal way. Their Wilson coefficients are power suppressed, and hence the series can be safely truncated. For convenience, we separate the perturbative contribution from the condensate part of the OPE:

$$\Pi_{\text{OPE}}(q^2) = \Pi_{\text{pert}}(q^2) + \Pi_{\text{cond}}(q^2). \quad (3.12)$$

To use the quark-hadron duality approximation, we replace the perturbative part by its dispersion representation, similar to the one in Eq. (3.4). The corresponding spectral density at leading order in α_s reads

$$\rho_{\text{pert}}^{\text{LO}}(s) = \frac{3}{8\pi^2 s} (m_c - m_d)^2 (s - (m_c + m_d)^2) \lambda^{1/2}(s, m_c^2, m_d^2) \theta(s - (m_c + m_d)^2).$$

Here, the light-quark mass dependence, which is important for the s -quark case, is exact as opposed to the expanded expressions in m_s that are given usually in the literature. For the next-to-leading order correction of $O(\alpha_s)$ it is possible to use previous calculations of this correlator from the literature, see e.g., Ref. [12]. We find it more convenient and straightforward to use the formula from Ref. [13] (see Eq. (A.2) therein), where the correlator of two pseudoscalar heavy-light currents was calculated. Performing the replacement $m_d \rightarrow -m_d$, we adapt this formula to our case of scalar currents.

In the same way, using Eqs. (B.6),(B.14) and (B.15) of Ref. [13], we obtain the condensate part of Eq. (3.12), including the $d = 3$ quark-condensate contribution (up to $O(\alpha_s)$), as well as the gluon, quark-gluon and four-quark condensate contributions with $d = 4, 5$ and 6 , respectively. All these formulas have been obtained for a nonvanishing light-quark mass. After Borel transform, the OPE (3.12) for the correlator in the adopted approximation becomes

$$\Pi_{\text{OPE}}(M^2) = \int_0^\infty ds e^{-s/M^2} \left[\rho_{\text{pert}}^{\text{LO}}(s) + \frac{\alpha_s}{\pi} \rho_{\text{pert}}^{\text{NLO}}(s) \right] + \Pi_{\text{cond}}(M^2). \quad (3.13)$$

The analogous result for the correlator Π^s can be achieved with obvious replacements in the formulas discussed above.

3.3 Sum rules and numerical results for decay constants

To finally obtain the two-point QCD sum rule, we equate the two Borel transformed analytical expressions for the correlator: the hadronic dispersion relation (3.4) and the result of the OPE calculation in Eq. (3.13). Semi-global quark-hadron duality is then used to remove the contributions of the continuum and excited states in the hadronic part of this equation. This assumption consists in equating the integrated spectral density ρ_{cont} in Eq. (3.4) to the integrated OPE spectral density:

$$\int_{s_{\text{th}}}^\infty ds \rho_{\text{cont}}(s) e^{-s/M^2} = \int_{s_0}^\infty ds \rho_{\text{OPE}}(s) e^{-s/M^2}, \quad (3.14)$$

where s_0 is an effective threshold, not necessarily equal to s_{th} .

Applying this procedure, we obtain the sum rules for the decay constants defined in Eq. (3.3) in the scenario 1:

$$f_{D_0^*}^2 m_{D_0^*}^4 \mathcal{E}(\Gamma_{D_0^*}, M^2, s_0) = \Pi_{\text{OPE}}(M^2, s_0), \quad (3.15)$$

and in the scenario 2:

$$f_{D_0^*}^2 m_{D_0^*}^4 e^{-m_{D_0^*}^2/M^2} = \Pi_{\text{OPE}}(M^2, s_0), \quad (3.16)$$

$$f_{D_0^{*'}}^2 (m_{D_0^*}^2 - m_{D_0^{*'}}^2) m_{D_0^{*'}}^4 e^{-m_{D_0^{*'}}^2/M^2} = \mathcal{D} \Pi_{\text{OPE}}(M^2, s_0'). \quad (3.17)$$

The functions $\mathcal{E}(\Gamma_{D_0^*}, M^2, s_0)$ and $\Pi_{\text{OPE}}(M^2, s_0)$ are equal to those defined in Eqs. (3.7) and (3.13), respectively, but with the upper limits of integrals taken at s_0 , reflecting the use of quark-hadron duality.

Parameter	Central value \pm Uncertainty/Interval	Ref.
normalisation scale	$\mu = [1.3, 2.5] \text{ GeV}$	[11, 14]
s -quark mass	$m_s(\mu = 2 \text{ GeV}) = 93.4_{-3.4}^{+8.6} \text{ MeV}$	[4]
c -quark mass	$m_c(\mu = 1.5 \text{ GeV}) = 1.205 \pm 0.035 \text{ GeV}$	[4]
strong coupling	$\alpha_s(\mu = 1.5 \text{ GeV}) = 0.353 \pm 0.006$	[4]
quark condensate	$\langle \bar{q}q \rangle(\mu = 1.5 \text{ GeV}) = -(0.278 \pm 0.022 \text{ GeV})^3$	[15]
s -quark condensate	$\langle \bar{s}s \rangle / \langle \bar{q}q \rangle = 0.8 \pm 0.3$	[16]
ratio $\langle \bar{q}Gq \rangle / \langle \bar{q}q \rangle$	$m_0^2 = 0.8 \pm 0.2 \text{ GeV}^2$	[16]
gluon condensate	$\langle GG \rangle = 0.012_{-0.012}^{+0.006} \text{ GeV}^4$	[16]
four-quark condensate	$r_{vac} = 0.5$	[16]

Table 2: Numerical inputs used for the decay constants calculation.

All the input parameters needed for the numerical evaluation of these sum rules are listed in Table 2 except for the Borel parameter M^2 and the effective thresholds $s_0^{(l)}$, which require a dedicated discussion. On the one hand, the Borel parameter has to be chosen large enough, such that higher power corrections in the OPE are sufficiently suppressed. On the other hand, the same parameter has to be chosen such small enough, that the contribution of continuum and excited states is subleading compared to the one of the lowest resonance. We found that these two requirements are satisfied in the range

$$M^2 = [3.0, 4.0] \text{ GeV}^2, \quad (3.18)$$

and also in this range the sum rules have a mild dependence on M^2 . The resulting variation is included in our uncertainty estimate.

The effective threshold $s_0^{(l)}$ is determined using the following standard procedure: we take the derivative of each sum rule (3.15)-(3.17) with respect to $-1/M^2$ and divide the result by the corresponding initial sum rule, obtaining:

$$m_{D_0^*}^2 = \frac{\frac{d}{d(-1/M^2)} \Pi_{\text{OPE}}(M^2, s_0)}{\Pi_{\text{OPE}}(M^2, s_0)}, \quad (3.19)$$

$$m_{D_0^{*'}}^2 = \frac{\frac{d}{d(-1/M^2)} \mathcal{D} \Pi_{\text{OPE}}(M^2, s_0')}{\mathcal{D} \Pi_{\text{OPE}}(M^2, s_0')}. \quad (3.20)$$

The effective threshold is then fixed by demanding that these constraints are fulfilled. In this procedure, we neglect the width of D_0^* , hence Eq. (3.19) for the lowest scalar resonance holds for both scenarios.

Using the D_0^* and $D_0^{*'}$ masses in Table 1, the inputs in Table 2 and the Borel window in Eq. (3.18) we find, for scenario 1,

$$s_0 = 6.84 \pm 0.89 \text{ GeV}^2, \quad (3.21)$$

and, for scenario 2,

$$s_0 = 5.50 \pm 0.72 \text{ GeV}^2, \quad (3.22)$$

$$s'_0 = 7.80 \pm 0.51 \text{ GeV}^2. \quad (3.23)$$

We can now obtain the numerical values for the decay constants. Evaluating the sum rule (3.15) (scenario 1) we find

$$f_{D_0^*} = 182 \pm 22 \text{ MeV}, \quad (3.24)$$

while the corresponding sum rules (3.16)-(3.17) (scenario 2) yield

$$f_{D_0^*} = 146 \pm 17 \text{ MeV}, \quad (3.25)$$

$$f_{D_0^{*'}} = 170 \pm 38 \text{ MeV}, \quad (3.26)$$

respectively. The quoted uncertainties are parametric and are obtained varying all input parameters independently. We can compare our result (3.24) for scenario 1 with a considerably earlier two-point sum rule prediction in Ref. [2], $m_{D_0^*} = 2.5 \pm 0.1 \text{ GeV}$, $f_{D_0^*} = 170 \pm 20 \text{ MeV}$ which is in the same ballpark.²

We also perform a numerical analysis for the charmed strange meson $D_{s_0}^*$ which is well identified independent of the scenario adopted for its nonstrange counterparts. Adapting the sum rule (3.15) to the $D_{s_0}^*$ meson case, we obtain

$$s_0 = 6.50 \pm 0.83 \text{ GeV}^2, \quad (3.27)$$

$$f_{D_{s_0}^*} = 123 \pm 21 \text{ MeV}. \quad (3.28)$$

Note that from an earlier sum rule calculation of this decay constant in Ref. [17] a similar result was obtained, albeit with small differences in the input parameters. Also in that paper, a different charmed-strange scalar current is used, without a quark mass prefactor, and hence the result should be scale-dependent.

Finally, let us comment on the difference between the decay constants of charmed-strange and charmed-nonstrange scalar mesons. The fact that the former decay constant is smaller than the latter, opposite to the case of charmed pseudoscalar mesons (see e.g. [13]), partly reflects the different relative sign of the s -quark mass in the prefactor of the interpolating current and in the OPE formulas. In addition, we notice that the difference between $f_{D_0^*}$ in scenario 1 and $f_{D_{s_0}^*}$ is unnaturally large for a typical $SU(3)$ flavour violation. A part of this effect is due to the effective increase of duality threshold by a relatively large D_0^* mass used as an input. Additional increase of $f_{D_{s_0}^*}$ is due to the fact that in scenario 1 the D_0^* is a broad state and hence the sum rule contains the width factor (3.7) which — given the large width of D_0^* — is smaller than a simple Borel exponent for a narrow resonance. In scenario 2, on the contrary, the $SU(3)$ flavour symmetry is violated within the expected 15 – 20%. In this respect, this scenario in which, as we already discussed, the lighter D_0^* state seems to be a more natural $SU(3)$ partner of D_{s_0} , seems more plausible.

4 LCSR for the $B_{(s)} \rightarrow D_{(s)0}^*$ form factors

We obtain the LCSRs for the $B \rightarrow D_0^*$ and $B_s \rightarrow D_{s_0}^*$ form factors from the following correlator which is a time-ordered product of the two currents sandwiched between the $B_{(s)}$ and vacuum

²One should keep in mind that the input parameters including the c -quark mass were at that time different.

states:

$$\begin{aligned}\mathcal{F}_\mu(p, q) &= i \int d^4x e^{ip \cdot x} \langle 0 | \mathcal{T} \left\{ J_{(s)}^\dagger(x), J_\mu^A(0) \right\} | \bar{B}_{(s)}(p+q) \rangle \\ &\equiv i p_\mu \mathcal{F}^{(p)}(p^2, q^2) + i q_\mu \mathcal{F}^{(q)}(p^2, q^2),\end{aligned}\quad (4.1)$$

where $J_{(s)}^\dagger$ is the conjugate of the scalar current (3.2) with four-momentum p and $J_\mu^A = \bar{c} \gamma_\mu \gamma_5 b$ is the axial part of the weak current with four-momentum q . The vector-current part of the transition matrix element between B and a scalar meson vanishes due to the P -parity conservation. With our four-momenta assignment, the momentum of the B -meson state is $p+q$, so that $(p+q)^2 = m_B^2$. The r.h.s. of Eq. (4.1) contains a decomposition of the correlation function in two Lorentz structures which we have simply chosen to be equal to the two independent four-momenta.

In this section, for definiteness we obtain LCSR for the $\bar{B}_0 \rightarrow D_0^{*+}$ form factors. The results for the transition of B^- into a neutral D_0^* are the same in the isospin symmetry limit. The LCSRs for $\bar{B}_s \rightarrow D_{s0}^+$ form factors are obtained by replacing the non-strange heavy mesons by their strange counterparts. As we shall see, in the adopted approximation for LCSRs, we have to replace the meson masses and the parameters of B -meson DAs, and all of them only implicitly depend on m_s . Explicitly, the s -quark mass only enters the normalisation factor of the charmed scalar current.

In the rest of this section, we present the hadronic dispersion relation for the correlator (4.1) in Subsection 4.1, while we perform the OPE calculation of the same correlator in Subsection 4.2. We derive the LCSRs and obtain the corresponding numerical results in Subsection 4.3.

4.1 Hadronic dispersion relation

The hadronic matrix element of the $B \rightarrow D_0^*$ transition is decomposed into two form factors in two different ways:

$$\begin{aligned}\langle D_0^*(p) | J_\mu^A | \bar{B}(p+q) \rangle &= i(2p_\mu + q_\mu) f_+^{BD_0^*}(q^2) + i q_\mu f_-^{BD_0^*}(q^2) \\ &= i \left(2p_\mu - \frac{m_B^2 - m_{D_0^*}^2 - q^2}{q^2} q_\mu \right) f_+^{BD_0^*}(q^2) + i \frac{m_B^2 - m_{D_0^*}^2}{q^2} q_\mu f_0^{BD_0^*}(q^2),\end{aligned}\quad (4.2)$$

where $f_0^{BD_0^*}$ is related to $f_\pm^{BD_0^*}$ via:

$$f_0^{BD_0^*}(q^2) = f_+^{BD_0^*}(q^2) + \frac{q^2}{m_B^2 - m_{D_0^*}^2} f_-^{BD_0^*}(q^2),\quad (4.3)$$

so that $f_0^{BD_0^*}(0) = f_+^{BD_0^*}(0)$. These definitions and relations are analogous to the standard ones for the $B \rightarrow D$ vector and scalar form factors of the vector weak current. In our case, the vector current is replaced by the axial one and the pseudoscalar meson is replaced by the scalar one. Similarly, the form factor $f_0^{BD_0^*}(q^2)$ can be expressed as the $B \rightarrow D_0^*$ matrix element of the pseudoscalar current:

$$f_0^{BD_0^*}(q^2) = \frac{m_b + m_c}{m_B^2 - m_{D_0^*}^2} \langle D_0^*(p) | \bar{c} i \gamma_5 b | \bar{B}(p+q) \rangle.\quad (4.4)$$

Scenario 1

To obtain the hadronic dispersion relation for the correlation function (4.1), we write down the imaginary part of it in the variable $p^2 = s$ for $s > 0$ and fixed q^2 :

$$\text{Im}_{p^2} \mathcal{F}_\mu(p, q) = \pi \delta(s - m_{D_0^*}^2) \langle 0 | J^\dagger | D_0^*(p) \rangle \langle D_0^*(p) J_\mu^A | \bar{B}(p+q) \rangle + \pi \hat{\rho}_{\text{cont}, \mu}(p, q) \theta(s - s_{\text{th}}). \quad (4.5)$$

As discussed in Subsection 3.1, $s_{\text{th}} = (m_D + m_\pi)^2$ and we isolate the lowest D_0^* pole (temporarily neglecting its total width). We also denote by $\hat{\rho}_{\text{cont}, \mu}$ the spectral density of continuum and excited states with the D_0^* quantum numbers. For this spectral density we use the same decomposition in invariant functions as in Eq. (4.1):

$$\hat{\rho}_{\text{cont}, \mu}(p, q) = p_\mu \hat{\rho}_{\text{cont}}^{(p)}(s, q^2) + q_\mu \hat{\rho}_{\text{cont}}^{(q)}(s, q^2).$$

Substituting the decomposition (4.2) and the decay constant definition (3.3) into Eq. (4.5) and separating the two kinematical structures according to Eq. (4.1), we obtain hadronic dispersion relations for the two invariant amplitudes:

$$\begin{aligned} \mathcal{F}^{(p)}(p^2, q^2) &= \frac{1}{\pi} \int_{s_{\text{th}}}^{\infty} ds \frac{\text{Im}_{p^2} \mathcal{F}^{(p)}(s, q^2)}{s - p^2} = \frac{2m_{D_0^*}^2 f_{D_0^*} f_+^{BD_0^*}(q^2)}{m_{D_0^*}^2 - p^2} + \int_{s_{\text{th}}}^{\infty} ds \frac{\hat{\rho}_{\text{cont}}^{(p)}(s, q^2)}{s - p^2}, \\ \mathcal{F}^{(q)}(p^2, q^2) &= \frac{1}{\pi} \int_0^{\infty} ds \frac{\text{Im}_{p^2} \mathcal{F}^{(q)}(s, q^2)}{s - p^2} = \frac{m_{D_0^*}^2 f_{D_0^*} [f_+^{BD_0^*}(q^2) + f_-^{BD_0^*}(q^2)]}{m_{D_0^*}^2 - p^2} + \int_{s_{\text{th}}}^{\infty} ds \frac{\hat{\rho}_{\text{cont}}^{(q)}(s, q^2)}{s - p^2}. \end{aligned} \quad (4.6)$$

Their Borel transform yields

$$\mathcal{F}^{(p)}(\hat{M}^2, q^2) = 2m_{D_0^*}^2 f_{D_0^*} f_+^{BD_0^*}(q^2) e^{-m_{D_0^*}^2/M^2} + \int_{s_{\text{th}}}^{\infty} ds \hat{\rho}_{\text{cont}}^{(p)}(s, q^2) e^{-s/M^2}, \quad (4.8)$$

$$\mathcal{F}^{(q)}(\hat{M}^2, q^2) = m_{D_0^*}^2 f_{D_0^*} [f_+^{BD_0^*}(q^2) + f_-^{BD_0^*}(q^2)] e^{-m_{D_0^*}^2/M^2} + \int_{s_{\text{th}}}^{\infty} ds \hat{\rho}_{\text{cont}}^{(q)}(s, q^2) e^{-s/M^2}. \quad (4.9)$$

Similar to the case of two-point sum rules (see Subsection 3.1), we improve the accuracy of these relations by introducing the s -dependent total width of D_0^* , i.e., by performing the replacement (3.7).

Scenario 2

In scenario 2, the hadronic dispersion relation $\mathcal{F}^{(i)}$ for the lowest-lying scalar resonance has the same form of Eqs. (4.8)-(4.9) but with different mass and decay constant of D_0^* . The second scalar resonance $D_0^{*'}$ can be isolated using again the operator (3.10), which yields

$$\begin{aligned} \mathcal{D}\mathcal{F}^{(p)}(\hat{M}^2, q^2) &= 2(m_{D_0^*}^2 - m_{D_0^{*'}}^2) m_{D_0^{*'}}^2 f_{D_0^{*'}} f_+^{BD_0^{*'}}(q^2) e^{-m_{D_0^{*'}}^2/M^2} \\ &+ \int_{s_{\text{th}}}^{\infty} ds (m_{D_0^*}^2 - s) \hat{\rho}_{\text{cont}}^{(p)}(s, q^2) e^{-s/M^2}, \end{aligned} \quad (4.10)$$

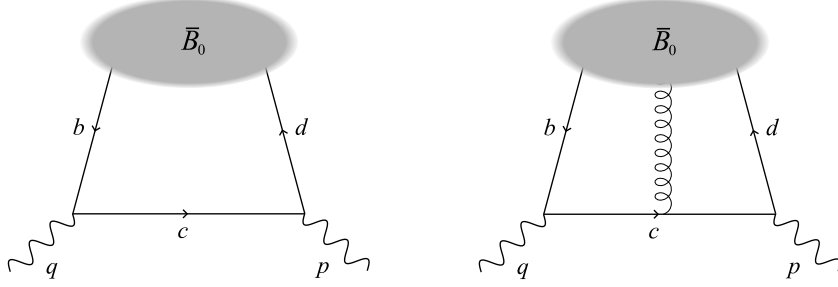


Figure 1: *The leading order (left panel) and soft gluon emission (right panel) diagrams for the correlation function (4.1).*

$$\begin{aligned} \mathcal{DF}^{(q)}(\hat{M}^2, q^2) &= (m_{D_0^*}^2 - m_{D_0^{*'}}^2) m_{D_0^{*'}}^2 f_{D_0^{*'}} [f_+^{BD_0^{*'}}(q^2) + f_-^{BD_0^{*'}}(q^2)] e^{-m_{D_0^{*'}}^2/M^2} \\ &+ \int_{s_{\text{th}}}^{\infty} ds (m_{D_0^*}^2 - s) \hat{\rho}_{\text{cont}}^{(q)}(s, q^2) e^{-s/M^2}, \end{aligned} \quad (4.11)$$

in analogy with Eq. (3.11) for the two-point sum rule.

4.2 Light-cone OPE for the correlator

For $p^2 \ll m_c^2$ and $q^2 \ll (m_b + m_c)^2$, that is far below the hadronic thresholds in the channels of the interpolating and weak currents, the correlator (4.1) can be calculated, expanding the time-ordered product of currents near the light-cone $x^2 \simeq 0$ [18]. In practical terms, we have to compute the diagrams depicted in Fig. 1. At leading order in α_s , the diagram on the left panel consists of the virtual c -quark propagating between the two vertices, whereas a quark-antiquark pair emitted at a light-cone separation forms a B -meson state. This long-distance part of the diagram is encoded in terms of the two-particle B -meson DAs defined in HQET. The computation of this diagram is described in detail in Ref. [1]. The only difference in our case is that the Dirac-structure in the vertex of the interpolation current has changed to a unit matrix.

In addition, to improve the accuracy of the light-cone OPE, we also take into account the effect of soft (low virtuality) gluon emitted from the c -quark line and absorbed, together with the quark-antiquark pair, in the three-particle B -meson DAs. The diagram is shown on the right panel of Fig. 1. To evaluate this diagram we need the one-gluon term in the light-cone expansion of the c -quark propagator [19]. For the latter, we use the most convenient symmetric form:

$$\langle 0 | T \{ c(x) \bar{c}(0) \} | 0 \rangle_G = -i \int_0^1 du G_{\mu\nu}(ux) \int \frac{d^4 f}{(2\pi)^4} e^{-ifx} \frac{\bar{u}(\not{f} + m_c) \sigma^{\mu\nu} + u \sigma^{\mu\nu} (\not{f} + m_c)}{2(f^2 - m_c^2)^2}, \quad (4.12)$$

where $G_{\mu\nu} = g_s G_{\mu\nu}^a (\lambda^a/2)$. This diagram, for a similar correlator, but with a different interpolating current, was computed earlier in Ref. [20], where the LCSRs for the $B \rightarrow D^{(*)}$ form

factors were obtained. In Ref. [21], the contributions of three-particle DAs to this sum rule were improved, taking into account a more complete set of three-particle B -meson DAs from Ref. [22] which we also use here. We will not present further details of our computation, referring e.g., to Ref. [23] where the contributions of three-particle DAs are also obtained and described for a similar correlator, but with the virtual s quark.

The OPE result for the invariant amplitudes $\mathcal{F}^{(i)}$ with $i = p, q$ can be reduced to the following generic form:

$$\mathcal{F}_{\text{OPE}}^{(i)}(p^2, q^2) = (m_c - m_d) m_B f_B \sum_{k=1}^4 \int_0^\infty d\sigma \frac{I^{(i,k)}(\sigma, q^2)}{(p^2 - s(\sigma, q^2))^k}, \quad (4.13)$$

where the variable

$$s(\sigma, q^2) = \sigma m_B^2 - \frac{\sigma q^2 - m_c^2}{1 - \sigma}, \quad (4.14)$$

is introduced, so that, inversely,

$$\sigma(s, q^2) = \frac{m_B^2 - q^2 + s - \sqrt{4(m_c^2 - s)m_B^2 + (m_B^2 - q^2 + s)^2}}{2m_B^2}. \quad (4.15)$$

The functions $I^{(i,k)}$ are defined as:

$$I^{(i,k)}(\sigma, q^2) = \sum_{\psi} \mathcal{C}_{\psi}^{(i,k)}(\sigma, q^2) \psi(\sigma m_B) + \sum_{\chi_j} \int_0^{\sigma m_B} d\omega_1 \int_{\sigma m_B - \omega_1}^{\infty} \frac{d\omega_2}{\omega_2} \mathcal{C}_{\chi_j}^{(i,k)}(\sigma, \omega_1, \omega_2, q^2) \chi_j(\omega_1, \omega_2), \quad (4.16)$$

where the first sum goes over the contributions of the four two-particle B -meson DAs:

$$\psi(\omega) = \left\{ \phi_+(\omega), \bar{\Phi}_{\pm}(\omega), g_+(\omega), \bar{G}_{\pm}(\omega) \right\},$$

and the second sum contains contributions of the eight linear combinations of three-particle DAs:

$$\chi_j(\omega_1, \omega_2) = \left\{ \chi_1(\omega_1, \omega_2), \dots, \chi_8(\omega_1, \omega_2) \right\}.$$

To derive Eq. (4.13) we have performed the replacement $\omega \mapsto \sigma m_B$ and $u \mapsto (\sigma m_B - \omega_1)/\omega_2$ for the coefficients of the two- and three-particle terms, respectively. The definitions of DAs and of their combinations are given in Appendix A, where we also specify their model and its parameters. We recall that the B -meson DAs are defined in HQET, i.e. in the limit $m_B \rightarrow \infty$, and the variables ω and $\omega_{1,2}$ are understood as the plus components of the momenta of light degrees of freedom inside B . This explains a formally infinite upper limit in Eq. (4.13). In reality, these variables are limited from above by $O(m_B)$, hence, the integration is supported only in the interval $0 < \omega < 1$. This is consistent with the exponential falloff of the model DAs adopted here and presented in Appendix A. The OPE in Eq. (4.13) is determined by the coefficients $\mathcal{C}_{\psi}^{(i,k)}$ and $\mathcal{C}_{\chi_j}^{(i,k)}$ entering Eq. (4.16). Our main analytical result are the expressions for these coefficients collected in Appendix B.

In order to use quark-hadron duality in the derivation of LCSRs, we need to recast the OPE (4.13) in the form of a dispersion integral in the variable p^2 . In addition, we perform the Borel transform with respect to p^2 . Following Ref. [21], the OPE result can be written as

$$\mathcal{F}_{\text{OPE}}^{(i)}(\hat{M}^2, q^2) = \mathcal{F}_{\text{OPE}}^{(i)}(\hat{M}^2, \hat{s}_0, q^2) + \mathcal{F}_{\text{OPE}}^{(i)}(\hat{M}^2, \infty, q^2), \quad (4.17)$$

where

$$\begin{aligned} \mathcal{F}_{\text{OPE}}^{(i)}(\hat{M}^2, \hat{s}_0, q^2) = & (m_c - m_d)m_B f_B \sum_{k=1}^4 \frac{(-1)^k}{(k-1)!} \left\{ \int_0^{\sigma_0} d\sigma e^{-s(\sigma, q^2)/\hat{M}^2} \frac{1}{(\hat{M}^2)^{k-1}} I^{(i,k)}(\sigma, q^2) \right. \\ & \left. + \left[e^{-s(\sigma, q^2)/\hat{M}^2} \sum_{j=1}^{k-1} \frac{1}{(\hat{M}^2)^{k-j-1}} \frac{1}{s'} \left(\frac{d}{d\sigma} \frac{1}{s'} \right)^{j-1} I^{(i,k)}(\sigma, q^2) \right]_{\sigma=\sigma_0} \right\} \end{aligned} \quad (4.18)$$

and

$$\mathcal{F}_{\text{OPE}}^{(i)}(\hat{M}^2, \infty, q^2) = (m_c - m_d)m_B f_B \sum_{k=1}^4 \frac{(-1)^k}{(k-1)!} \int_{\sigma_0}^{\infty} d\sigma e^{-s(\sigma, q^2)/\hat{M}^2} \left(\frac{d}{d\sigma} \frac{1}{s'} \right)^{k-1} I^{(i,k)}(\sigma, q^2). \quad (4.19)$$

Here, we have introduced the following notation:

$$\left(\frac{d}{d\sigma} \frac{1}{s'} \right)^n f(\sigma) \equiv \left(\frac{d}{d\sigma} \frac{1}{s'} \left(\frac{d}{d\sigma} \frac{1}{s'} \cdots f(\sigma) \right) \right), \quad s' \equiv \frac{ds}{d\sigma}, \quad \sigma_0 \equiv \sigma(\hat{s}_0, q^2).$$

The corresponding OPE expressions in the case of $B_s \rightarrow D_{s_0}^*$ form factors are obtained by replacing $(m_c - m_d) \rightarrow (m_c - m_s)$, $f_B \rightarrow f_{B_s}$ and $m_B \rightarrow m_{B_s}$ in Eq. (4.13).

4.3 Light-cone sum rules and numerical results for the form factors

The LCSRs for $B_{(s)} \rightarrow D_{(s_0)}^*$ form factors can now be easily obtained by equating the OPE results in Eq. (4.17) with the corresponding hadronic representations in Eqs. (4.8)-(4.11). The semi-global quark-hadron duality approximation is then used to remove the contributions of continuum and excited states. In other words we assume that the term denoted as $\mathcal{F}_{\text{OPE}}^{(i)}(\hat{M}^2, \infty, q^2)$ in Eq. (4.17) cancels the integral over the spectral density $\hat{\rho}_{\text{cont}}^{(i)}(s, q^2)$. Following these steps, we derive the sum rules for the form factors in scenario 1:

$$2m_{D_0^*}^2 f_{D_0^*} f_+^{BD_0^*}(q^2) \mathcal{E}(\Gamma_{D_0^*}, \hat{M}^2, \hat{s}_0) = \mathcal{F}_{\text{OPE}}^{(p)}(\hat{M}^2, \hat{s}_0, q^2), \quad (4.20)$$

$$m_{D_0^*}^2 f_{D_0^*} [f_+^{BD_0^*}(q^2) + f_-^{BD_0^*}(q^2)] \mathcal{E}(\Gamma_{D_0^*}, \hat{M}^2, \hat{s}_0) = \mathcal{F}_{\text{OPE}}^{(q)}(\hat{M}^2, \hat{s}_0, q^2), \quad (4.21)$$

and in scenario 2:

$$2m_{D_0^*}^2 f_{D_0^*} f_+^{BD_0^*}(q^2) e^{-m_{D_0^*}^2/\hat{M}^2} = \mathcal{F}_{\text{OPE}}^{(p)}(\hat{M}^2, \hat{s}_0, q^2), \quad (4.22)$$

$$m_{D_0^*}^2 f_{D_0^*} [f_+^{BD_0^*}(q^2) + f_-^{BD_0^*}(q^2)] e^{-m_{D_0^*}^2/\hat{M}^2} = \mathcal{F}_{\text{OPE}}^{(q)}(\hat{M}^2, \hat{s}_0, q^2), \quad (4.23)$$

Parameter	Central value \pm Uncertainty	Ref.
B -meson decay constant	$f_B = 190.0 \pm 1.3$ MeV	[15]
B_s -meson decay constant	$f_{B_s} = 230.3 \pm 1.3$ MeV	[15]
Parameters of the $B_{(s)}$ -meson DAs	$\lambda_B = 0.460 \pm 0.110$ GeV	[24]
	$\lambda_{B_s}/\lambda_B = 1.19 \pm 0.14$	[25]
	$\lambda_E^2 = 0.02 \pm 0.03$ GeV ²	[26, 27]
	$\lambda_H^2 = 0.11 \pm 0.08$ GeV ²	[26, 27]

Table 3: Numerical inputs used for the form factor calculation from LCSRs.

$$2(m_{D_0^*}^2 - m_{D_0^{*'}}^2)m_{D_0^{*'}}^2 f_{D_0^{*'}} f_+^{BD_0^{*'}}(q^2) e^{-m_{D_0^{*'}}^2/\hat{M}^2} = \mathcal{DF}_{\text{OPE}}^{(p)}(\hat{M}^2, \hat{s}'_0, q^2), \quad (4.24)$$

$$(m_{D_0^*}^2 - m_{D_0^{*'}}^2)m_{D_0^{*'}}^2 f_{D_0^{*'}} [f_+^{BD_0^{*'}}(q^2) + f_-^{BD_0^{*'}}(q^2)] e^{-m_{D_0^{*'}}^2/\hat{M}^2} = \mathcal{DF}_{\text{OPE}}^{(q)}(\hat{M}^2, \hat{s}'_0, q^2), \quad (4.25)$$

The input parameters needed to calculate the form factors from these sum rules are all listed in Table 3, with the exception of the quark masses that are in Table 2 and the decay constants of charmless scalar mesons that have been obtained in Section 3. In the adopted approximation for the OPE, the B -meson DAs entering the LCSRs are characterised by four parameters (see Appendix A for more details). One of them is the B -meson decay constant for which we adopt the lattice QCD average. The other three parameters include the first inverse moment λ_B and the normalisation parameters λ_E^2 and λ_H^2 of three-particle DAs, the latter defined as the vacuum-to- B matrix elements of local quark-antiquark-gluon-operators in HQET [28]. The values of all three parameters in Table 3 are taken from the QCD sum rule determinations. As a conservative choice, the intervals for the parameters λ_E^2 and λ_H^2 are obtained by averaging the central values obtained from the two independent sum rules in Refs. [26, 27] and adding their respective uncertainties. Given the large uncertainties of these two parameters, we take the same intervals also for the B_s -meson DAs. However, for λ_{B_s} we use the QCD sum rule estimates from Ref. [25], which is also consistent with the more recent independent calculation of this parameter in [29]. Furthermore, we find that the Borel parameter \hat{M}^2 of the LCSRs, which is in principle independent from the Borel parameter M^2 of the two-point sum rules, can be varied in the same interval of Eq. (3.18), i.e. between 3.0 GeV² and 4.0 GeV². In fact, we have checked that the LCSRs are stable in this interval and both the duality-estimated contribution of heavier states and the subleading twist contributions are sufficiently suppressed. Following Refs. [1, 23], we also use for the LCSRs the same threshold as the one determined in Subsection 3.3 for the two-point sum rules, that is, we fix $\hat{s}_0^{(l)} = s_0^{(l)}$.

For each LCSR considered above, we calculate the OPE expression $\mathcal{F}_{\text{OPE}}^{(i)}(\hat{M}^2, \hat{s}_0, q^2)$ or $\mathcal{DF}_{\text{OPE}}^{(i)}(\hat{M}^2, \hat{s}_0, q^2)$, in both cases denoted for brevity as $\mathcal{F}_{\text{OPE}}^{(i)}(q^2)$, where $i = p$ or q , at $q^2 = \{-20, -15, -10, -5\}$ GeV², varying all input parameters within their adopted intervals. Using the OPE only for negative q^2 values is justified by the fact that for $q^2 \geq 0$, the subleading twist contributions become numerically of the same order of magnitude as the leading twist ones at $q^2 = 0$. This behaviour is not surprising and has already been noticed in Ref. [1]. We also ob-

Process (scenario)	(i)	$\alpha_0^{(i)}$	$\alpha_1^{(i)}$	Correlation
$B \rightarrow D_0^* (1)$	(p)	-0.100 ± 0.060	0.15 ± 0.15	-0.93
	(q)	0.019 ± 0.021	-0.029 ± 0.085	-0.97
$B_s \rightarrow D_{s0}^* (1)$	(p)	-0.060 ± 0.051	0.050 ± 0.16	-0.97
	(q)	0.004 ± 0.017	0.029 ± 0.076	-0.98
$B \rightarrow D_0^* (2)$	(p)	-0.074 ± 0.053	0.13 ± 0.18	-0.97
	(q)	0.011 ± 0.018	-0.007 ± 0.080	-0.98
$B \rightarrow D_0^{*'} (2)$	(p)	0.090 ± 0.075	-0.27 ± 0.39	-0.85
	(q)	-0.051 ± 0.024	0.20 ± 0.12	-0.84

Table 4: Coefficients of the z - expansion (4.26) fitted to $\mathcal{F}_{\text{OPE}}^{(i)}$.

serve that the contributions of three-particle DAs to LCSRs are relatively small (of the order of few per cent) compared to the contributions of two-particle DAs, in agreement with the results of Refs. [21, 30].

To obtain the form factors in the semileptonic region, that is for $0 < q^2 < (m_{B(s)} - m_{D(s)0}^*)^2$, we fit for each LCSR the OPE results $\mathcal{F}_{\text{OPE}}^{(i)}(q^2)$ at $q^2 \leq 0$ to the following z expansion:

$$\mathcal{F}_{\text{fit}}^{(i)}(q^2) = \frac{1}{1 - \frac{q^2}{m_{(i)}^2}} \sum_{k=0}^K \alpha_k^{(i)} [z(q^2) - z(0)]^k. \quad (4.26)$$

The $q^2 \mapsto z$ map is defined as

$$z(q^2) = \frac{\sqrt{t_+ - q^2} - \sqrt{t_+ - t_0}}{\sqrt{t_+ - q^2} + \sqrt{t_+ - t_0}}, \quad (4.27)$$

where

$$t_+ = (m_B + m_D)^2, \quad t_0 = (m_B + m_D)(\sqrt{m_B} - \sqrt{m_D})^2. \quad (4.28)$$

The parameter $m_{(i)}$ in Eq. (4.26) is the mass of the lightest $b\bar{c}$ pole in the timelike region of the form factor related to $\mathcal{F}_{\text{OPE}}^{(i)}$ via LCSRs. In fact, $\mathcal{F}_{\text{OPE}}^{(p)}$ is associated with the form factor f_+ which contains $b\bar{c}$ states with spin-parity $J^P = 1^+$ in the timelike region. Similarly, $\mathcal{F}_{\text{OPE}}^{(q)}$ is related to a linear combination of f_+ and f_0 , and the latter form factor has lighter states with $J^P = 0^-$. Hence, we take $m_{(p)} = 6.767$ GeV and $m_{(q)} = 6.275$ GeV, since those are the masses of the lightest $b\bar{c}$ states with $J^P = 1^+$ and $J^P = 0^-$, respectively, as estimated in lattice QCD [31].

We only consider the first two terms in the parametrization (4.26), given the large uncertainties and correlations between the data points used. Our results for the $\alpha_k^{(i)}$ coefficients are summarised in Table 4. With these coefficients, we extrapolate the z -expansion (4.26) into the semileptonic region, and finally, via LCSR relations obtain the form factors in that region. Our numerical results for the form factors plotted as a function of q^2 are shown in Fig. 2. The central values, uncertainties and correlations of these form factors at any q^2 can be easily obtained

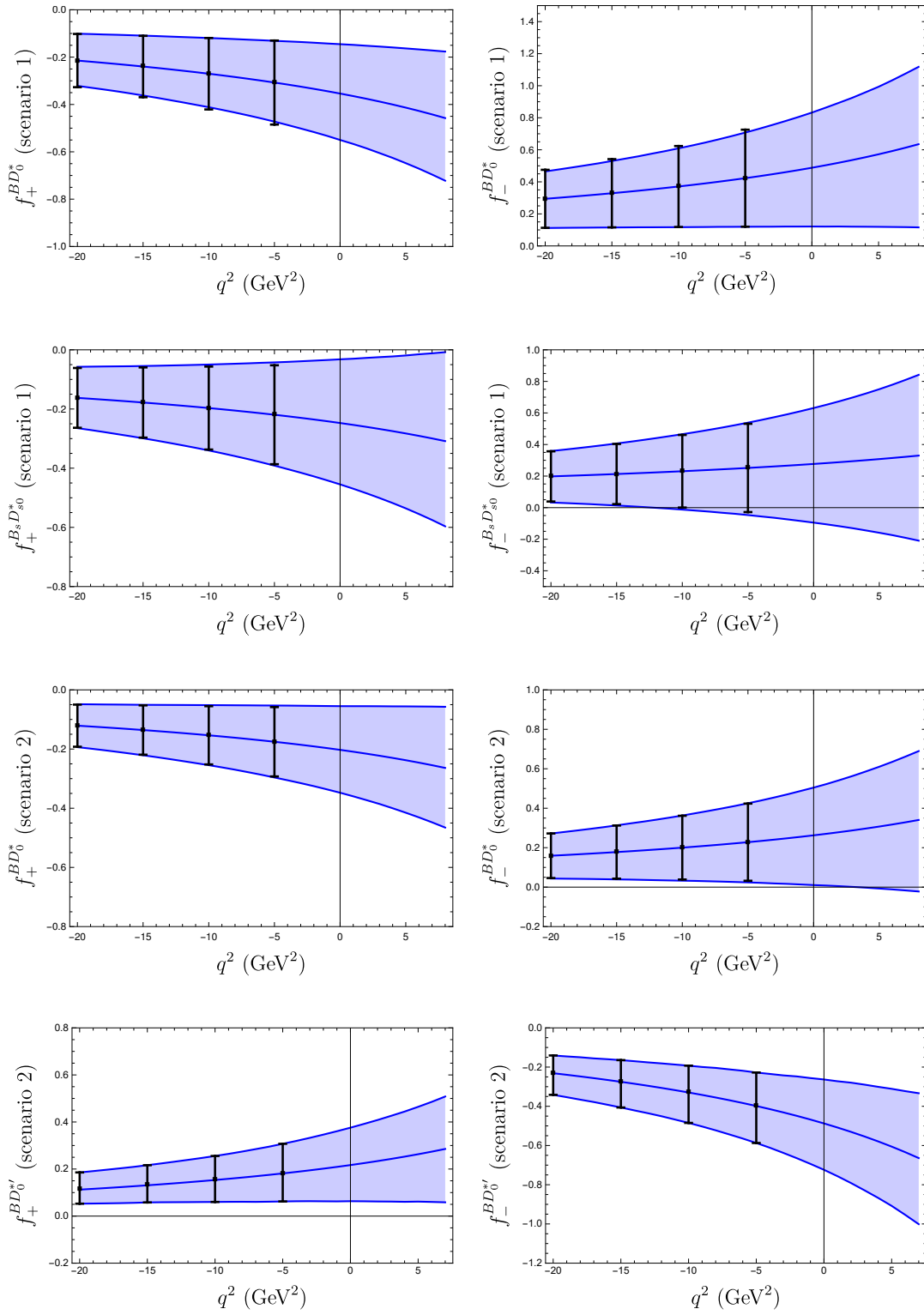


Figure 2: Form factors plotted as a function of q^2 . The intervals in black are the results of our LCSR calculation. The central values and 68% probability envelopes in blue are the results obtained from our fit to the z expansion in Eq. (4.26).

Process (scenario)	Form factor	$q^2 = 0$	$q^2 = \frac{1}{2}q_{\max}^2$	$q^2 = q_{\max}^2$
$B \rightarrow D_0^* (1)$	$f_+^{BD_0^*}$	$-0.35^{+0.20}_{-0.21}$	$-0.41^{+0.22}_{-0.25}$	$-0.48^{+0.26}_{-0.30}$
	$f_-^{BD_0^*}$	$0.49^{+0.34}_{-0.37}$	$0.57^{+0.40}_{-0.45}$	$0.67^{+0.47}_{-0.56}$
$B_s \rightarrow D_{s0}^* (1)$	$f_+^{BD_{s0}^*}$	$-0.24^{+0.21}_{-0.21}$	$-0.28^{+0.25}_{-0.25}$	$-0.32^{+0.29}_{-0.31}$
	$f_-^{BD_{s0}^*}$	$0.27^{+0.36}_{-0.37}$	$0.30^{+0.43}_{-0.45}$	$0.34^{+0.52}_{-0.56}$
$B \rightarrow D_0^* (2)$	$f_+^{BD_0^*}$	$-0.20^{+0.15}_{-0.14}$	$-0.23^{+0.18}_{-0.17}$	$-0.27^{+0.21}_{-0.21}$
	$f_-^{BD_0^*}$	$0.25^{+0.25}_{-0.24}$	$0.29^{+0.30}_{-0.30}$	$0.34^{+0.36}_{-0.37}$
$B \rightarrow D_0^{*'} (2)$	$f_+^{BD_0^{*}'}$	$0.22^{+0.16}_{-0.23}$	$0.25^{+0.19}_{-0.28}$	$0.30^{+0.23}_{-0.35}$
	$f_-^{BD_0^{*}'}$	$-0.49^{+0.24}_{-0.22}$	$-0.58^{+0.29}_{-0.28}$	$-0.70^{+0.35}_{-0.35}$

Table 5: *Form factor values at three selected q^2 points.*

from Eqs. (4.20)–(4.25), using the entries in Table 4 and the values of decay constants given in Section 3.3. In Table 5, for convenience of the reader, we give the values of the form factors at $q^2 = \{0, \frac{1}{2}q_{\max}^2, q_{\max}^2\}$, where $q_{\max}^2 = (m_B - m_{D_0^*})^2$.

The uncertainties of our calculation for $q^2 < 0$ further increase in the semileptonic region due to the extrapolation. The uncertainties of our LCSR results are mostly parametric and the main contribution to the error budget comes from the λ_B parameter. We stress that a better knowledge of this parameter would significantly improve the precision of the predictions from the LCSRs with B -meson DAs, including those obtained here.

Using our form factor results, we can obtain predictions for physical observables in, e.g., the semileptonic decays $B \rightarrow D_0^* \ell \bar{\nu}$, $B_s \rightarrow D_{s0}^* \ell \bar{\nu}$, and $B \rightarrow D_0^{*'} \ell \bar{\nu}$. We calculate the differential decay widths using the expressions in Ref. [32] and plot the results in Fig. 3 as a function of the variable

$$w = \frac{m_B^2 - m_{D_0^*}^2 - q^2}{2m_B m_{D_0^*}}.$$

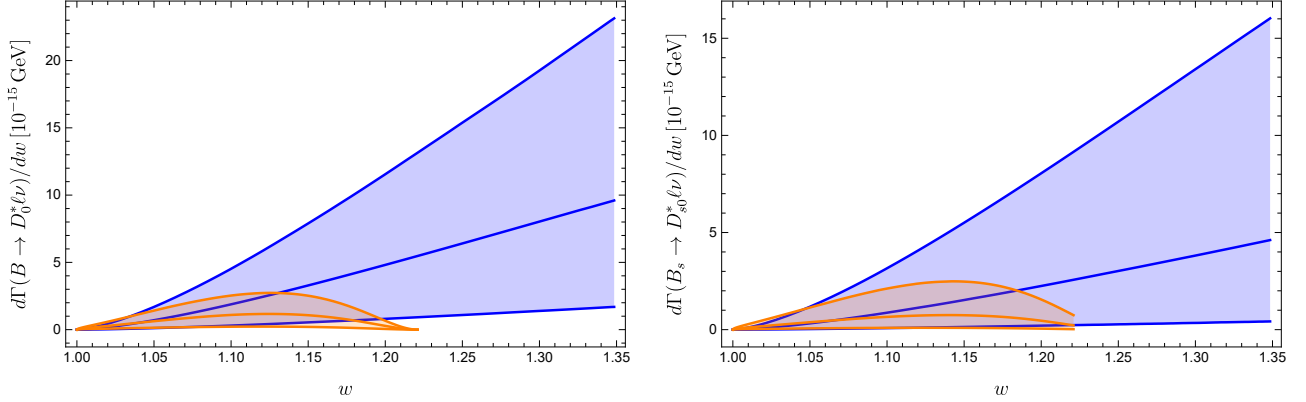
For the branching ratios we obtain for scenario 1

$$\begin{aligned}
\mathcal{B}(\bar{B}^0 \rightarrow D_0^* \ell \bar{\nu}) &= (3.6^{+5.1}_{-3.0}) \cdot 10^{-3}, \\
\mathcal{B}(\bar{B}^0 \rightarrow D_0^* \tau \bar{\nu}) &= (3.9^{+5.1}_{-3.1}) \cdot 10^{-4}, \\
\mathcal{B}(\bar{B}_s \rightarrow D_{s0}^* \ell \bar{\nu}) &= (1.9^{+3.8}_{-1.7}) \cdot 10^{-3}, \\
\mathcal{B}(\bar{B}_s \rightarrow D_{s0}^* \tau \bar{\nu}) &= (2.6^{+4.9}_{-2.2}) \cdot 10^{-4},
\end{aligned} \tag{4.29}$$

and for scenario 2

$$\begin{aligned}
\mathcal{B}(\bar{B}^0 \rightarrow D_0^* \ell \bar{\nu}) &= (1.6^{+3.2}_{-1.4}) \cdot 10^{-3}, \\
\mathcal{B}(\bar{B}^0 \rightarrow D_0^* \tau \bar{\nu}) &= (2.4^{+4.7}_{-2.1}) \cdot 10^{-4}, \\
\mathcal{B}(\bar{B}^0 \rightarrow D_0^{*'} \ell \bar{\nu}) &= (2.3^{+1.4}_{-1.8}) \cdot 10^{-3}, \\
\mathcal{B}(\bar{B}^0 \rightarrow D_0^{*'} \tau \bar{\nu}) &= (1.9^{+1.1}_{-1.4}) \cdot 10^{-4},
\end{aligned} \tag{4.30}$$

Scenario 1



Scenario 2

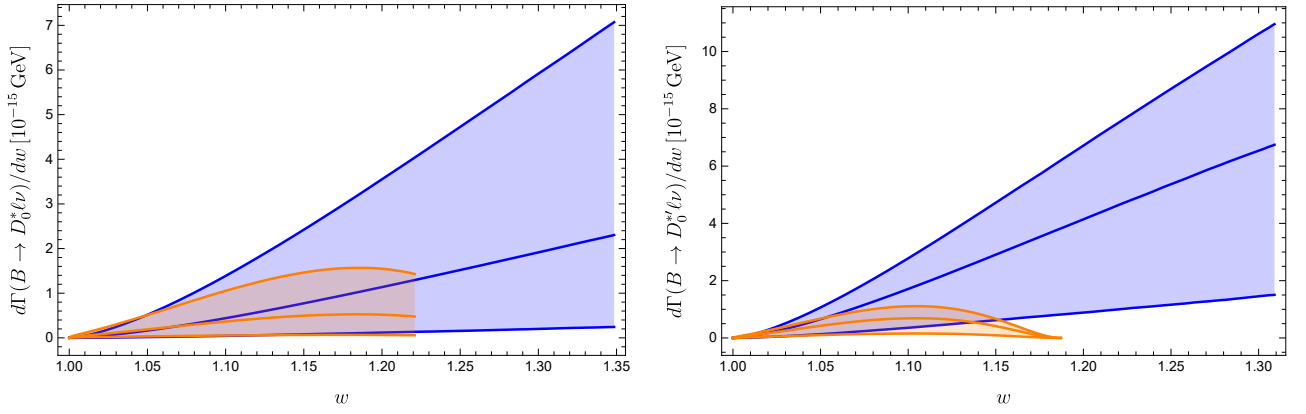


Figure 3: *Differential decay widths as a function of w . The blue (orange) bands are the 68% intervals for $\ell = e, \mu$ ($\ell = \tau$).*

with $l = e, \mu$. We also calculate the lepton flavor universality ratios defined as

$$R(D_0^*) = \frac{\Gamma(B \rightarrow D_0^* \tau \bar{\nu})}{\Gamma(B \rightarrow D_0^* \ell \bar{\nu})}, \quad (4.31)$$

for which we obtain in scenario 1

$$\begin{aligned} R(D_0^*) &= 0.11^{+0.03}_{-0.01}, \\ R(D_{s0}^*) &= 0.14^{+0.07}_{-0.02}, \end{aligned} \quad (4.32)$$

and in scenario 2

$$\begin{aligned} R(D_0^*) &= 0.16^{+0.04}_{-0.01}, \\ R(D_0^{*\prime}) &= 0.077^{+0.029}_{-0.010}. \end{aligned} \quad (4.33)$$

Clearly, in these ratios the theory uncertainties partially cancel and hence their relative uncertainties are much smaller than in the individual branching ratios. Our prediction for the branching ratio in scenario 1 agrees with the experimental average $\mathcal{B}(\bar{B}^0 \rightarrow D_0^*(2300)\ell\bar{\nu}) = (3.0 \pm 1.2) \cdot 10^{-3}$ of the Particle Data Group [4]. Also our prediction for $R(D_0^*)$ (again in scenario 1) is in a agreement with the data driven estimate of Ref. [32] (see also Ref. [33]). We find agreement between our results for the $B_s \rightarrow D_{s0}^* \ell \bar{\nu}$ branching ratio and the results of Ref. [34],

which were obtained with QCD sum rules in the framework of heavy quark effective field theory. There are no measurements or other theoretical predictions for the observables in the decays of scenario 2. In fact, our predictions are the first ones for such observables. With better experimental and theoretical precision, the semileptonic decay channels considered here could also be used as an alternative to the well studied $B \rightarrow D^{(*)}\ell\nu_\ell$ decays to probe the $b \rightarrow c\bar{\nu}$ transitions and to extract V_{cb} .

5 Conclusion

We have calculated the $B \rightarrow D_0^*$ form factors using for the first time the light-cones sum rules (LCSRs) with the B -meson distribution amplitudes (DAs). In this method, the c -quark mass is finite and the B -meson DAs are defined in HQET. This work is complementary to Ref. [1], where similar LCSRs have been applied to the B meson transitions to the axial charmed mesons. Here, we have also extended the computation to the $B_s \rightarrow D_{s0}^*$ processes taking into account the non-vanishing strange-quark mass. Our main analytical results are the novel expressions for the LCSRs involving light-cone OPE up to twist-four accuracy for B -meson DAs. At the same time, we have recalculated the decay constants of charmed scalar mesons from two-point QCD sum rules, which is an important update of earlier works.

The most acute problem related to the charmed scalar mesons is their identification as resonances in the $D\pi$ system. According to Particle Data Group [4], the ground-state meson with these quantum numbers is $D_0^*(2300)$ which is surprisingly heavy with respect to its strange counterpart $D_{s0}^*(2317)$. According to Ref. [6], the situation is markedly different and there are two charmed scalar resonances, $D_0^*(2105)$ and $D_0^*(2451)$, where the lightest one is the natural non-strange partner of $D_{s0}^*(2317)$. For the sake of completeness, we considered both the possibilities as two different scenarios, and obtained the $B \rightarrow D_0^*$ form factors and the D_0^* decay constants for each scenario independently.

We have calculated the form factor for $q^2 < 0$ and extrapolated these results to the semileptonic region of the phase space using a z expansion. Our form factor results have sizeable uncertainties, which are mostly due to the poorly known parameters of the B -meson DAs. We use these results to predict observables for the semileptonic $\bar{B} \rightarrow D_0^*\ell\bar{\nu}_\ell$ decays. Our predictions agree with experimental measurements where available. We also predict observables in the $\bar{B}_s \rightarrow D_{s0}^*\ell\bar{\nu}_\ell$ decays.

Furthermore, the results obtained in this paper allow us to make one more step towards filling the observed gap between the inclusive $b \rightarrow c\ell\nu_\ell$ decay rate of B meson and the sum over exclusive decay contributions to this rate. Having at hand the predictions for the partial widths of $B \rightarrow D_1^*\ell\nu_\ell$ and $B \rightarrow D_0^*\ell\nu_\ell$, respectively, from Ref. [1] and from this paper, we can calculate their ratios to the widths of the dominant $B \rightarrow D^{(*)}\ell\nu_\ell$ modes, using the LCSR results obtained for the form factors of the latter modes, e.g. from Ref. [21]. These ratios, due to partial cancellation of DA parameters, will be then more accurate than our predictions for the individual widths. Combining the ratios with the well measured $B \rightarrow D^{(*)}\ell\nu_\ell$ widths will enable us to estimate the share of semileptonic B decays into charmed axial and scalar mesons in the inclusive rate. This type of analysis goes beyond our scope and will be done elsewhere.

We emphasise that in order to make further progress in the B decays involving the scalar charmed mesons, it is crucial to have a better knowledge of their spectrum. Currently, the

main information on this spectrum comes from the studies of the three-body nonleptonic decay $B \rightarrow D\pi\pi$, identifying D_0^* resonances in the $D\pi$ two-body subsystem of the final state. Needless to say, in future the final word on this spectroscopy should come from the semileptonic decays $B \rightarrow D\pi\ell\nu_\ell$ where a careful analysis of the observables should help to finally establish the mass of the lightest D_0^* . Our results on $B \rightarrow D_0^*$ form factors obtained in this paper can help to analyse and resolve this problem.

Acknowledgements

This research was supported by the Deutsche Forschungsgemeinschaft (DFG, German Research Foundation) under grant 396021762 - TRR 257 ‘‘Particle Physics Phenomenology after the Higgs Discovery’’. R.M. acknowledges the support of this grant via Mercator Fellowship and the hospitality during the visit at Universitat Siegen.

A Light-Cone DAs of B -meson

The definitions and twist expansion of the B -meson light-cone distribution amplitudes are taken from Ref. [22]. These amplitudes are defined in HQET introducing the four-velocity $v = (p + q)/m_B$ of the B -meson with $v = (1, \vec{0})$ in its rest frame. For the two-particle DAs we use

$$\langle 0 | \bar{q}^\alpha(x) h_v^\beta(0) | \bar{B}(v) \rangle = -\frac{if_B m_B}{4} \int_0^\infty d\omega \left\{ (1 + \psi) \left[\phi_+(\omega) - g_+(\omega) \partial_\lambda \partial^\lambda \right. \right. \\ \left. \left. + \frac{1}{2} (\bar{\Phi}_\pm(\omega) - \bar{G}_\pm(\omega) \partial_\lambda \partial^\lambda) \gamma^\rho \partial_\rho \right] \gamma_5 \right\}^{\beta\alpha} e^{-il \cdot x} \Big|_{l=\omega v}. \quad (\text{A.1})$$

Here we have defined $\partial_\mu \equiv \partial/\partial l^\mu$ and

$$\bar{\Phi}_\pm(\omega) \equiv \int_0^\omega d\tau (\phi_+(\tau) - \phi_-(\tau)), \quad \bar{G}_\pm(\omega) \equiv \int_0^\omega d\tau (g_+(\tau) - g_-(\tau)), \quad (\text{A.2})$$

where the DAs of twist-two, three and twist-four, respectively, ϕ_+ , ϕ_- and g_+ , are taken into account. Consistently with Ref. [1], we also take into account g_- , which is formally a twist-five contribution, in the Wandzura-Wilczek (WW) limit. Eq. (A.1) is equivalent to the definition in a form of x^2 expansion in Ref. [22] (see Eq.(4.1) therein), and at the same time has some practical advantages, e.g. the barred functions (A.2) are explicitly present. In our convention, the B -meson decay constant f_B in the above definition is defined in full QCD and the state $|B(v)\rangle$ has a relativistic normalisation.

For the three-particle DAs up to twist-four we use:

$$\langle 0 | \bar{q}(x) G_{\mu\nu}(ux) \Gamma^{\mu\nu} h_v(0) | \bar{B}(v) \rangle = \frac{f_B m_B}{4} \int_0^\infty d\omega_1 d\omega_2 e^{-i(\omega_1 + u\omega_2)v \cdot x} \\ \text{Tr} \left\{ \gamma_5 \Gamma^{\mu\nu} (1 + \psi) \left[(v_\mu \gamma_\nu - v_\nu \gamma_\mu) \phi_3 + \frac{i}{2} \sigma_{\mu\nu} [\phi_3 - \phi_4] + \frac{x_\mu v_\nu - x_\nu v_\mu}{2v \cdot x} [\phi_3 + \phi_4 - 2\psi_4] \right] \right\}$$

$$\begin{aligned}
& -\frac{x_\mu\gamma_\nu - x_\nu\gamma_\mu}{2v \cdot x} [\phi_3 + \tilde{\psi}_4] + \frac{i\epsilon_{\mu\nu\alpha\beta}x^\alpha v^\beta}{2v \cdot x} \gamma_5 [\phi_3 - \phi_4 + 2\tilde{\psi}_4] - \frac{i\epsilon_{\mu\nu\alpha\beta}x^\alpha}{2v \cdot x} \gamma^\beta \gamma_5 [\phi_3 - \phi_4 + \tilde{\psi}_4] \\
& -\left. \frac{(x_\mu v_\nu - x_\nu v_\mu)\not{x}}{2(v \cdot x)^2} [\phi_4 - \psi_4 - \tilde{\psi}_4] - \frac{(x_\mu\gamma_\nu - x_\nu\gamma_\mu)\not{x}}{4(v \cdot x)^2} [\phi_3 - \phi_4 + 2\tilde{\psi}_4] \right\}, \tag{A.3}
\end{aligned}$$

where $\Gamma^{\mu\nu}$ is an arbitrary Dirac matrix. In the above, the functional dependence $\phi_3 = \phi_3(\omega_1, \omega_2)$, etc., is not shown for brevity, and the index 3,4 indicates the twist of the DAs. Also, the Wilson lines are implied but not shown explicitly on l.h.s. of both Eqs. (A.1), (A.3). This form of the matrix element has been obtained from the one in Ref. [22] by defining $x_\mu = z_1 n_\mu$ and $u = z_2/z_1$.

We also introduce the notation for the once and twice integrated three-particle DAs:

$$\bar{\Phi}(\omega_1, \omega_2) = \int_0^{\omega_1} d\tau \Phi(\tau, \omega_2), \quad \overline{\overline{\Phi}}(\omega_1, \omega_2) = \int_0^{\omega_1} d\tau \overline{\overline{\Phi}}(\tau, \omega_2), \tag{A.4}$$

where $\Phi = \{\phi_3, \phi_4, \psi_4, \tilde{\psi}_4\}$. The integrated functions defined above enter the OPE expressions, in particular the linear combinations of the three-particle DAs multiplying the OPE coefficients in Eq. (4.16). These combinations are defined as:

$$\begin{aligned}
\chi_1(\omega_1, \omega_2) &\equiv \phi_3(\omega_1, \omega_2), \\
\chi_2(\omega_1, \omega_2) &\equiv \phi_3(\omega_1, \omega_2) - \phi_4(\omega_1, \omega_2), \\
\chi_3(\omega_1, \omega_2) &\equiv \bar{\phi}_3(\omega_1, \omega_2) + \bar{\phi}_4(\omega_1, \omega_2) - 2\bar{\psi}_4(\omega_1, \omega_2), \\
\chi_4(\omega_1, \omega_2) &\equiv \bar{\phi}_3(\omega_1, \omega_2) + \bar{\psi}_4(\omega_1, \omega_2), \\
\chi_5(\omega_1, \omega_2) &\equiv \bar{\phi}_3(\omega_1, \omega_2) - \bar{\phi}_4(\omega_1, \omega_2) + 2\bar{\psi}_4(\omega_1, \omega_2), \\
\chi_6(\omega_1, \omega_2) &\equiv \bar{\phi}_3(\omega_1, \omega_2) - \bar{\phi}_4(\omega_1, \omega_2) + \bar{\psi}_4(\omega_1, \omega_2), \\
\chi_7(\omega_1, \omega_2) &\equiv \bar{\bar{\phi}}_3(\omega_1, \omega_2) - \bar{\bar{\phi}}_4(\omega_1, \omega_2) - \bar{\bar{\psi}}_4(\omega_1, \omega_2), \\
\chi_8(\omega_1, \omega_2) &\equiv \bar{\bar{\phi}}_3(\omega_1, \omega_2) - \bar{\bar{\phi}}_4(\omega_1, \omega_2) + 2\bar{\bar{\psi}}_4(\omega_1, \omega_2), \tag{A.5}
\end{aligned}$$

where the single- and double-barred functions entering $\chi_{3-8}(\omega_1, \omega_2)$ are defined in Eq. (A.4).

In the numerical analysis, we use the exponential model (Model-I) proposed in Ref. [22].³ It stems from the ansatz adopted for two-particle DAs in Ref. [28] and extended to three-particle DAs in Ref. [18]:

$$\phi_+(\omega) = \frac{\omega}{\lambda_B^2} e^{-\omega/\lambda_B}, \tag{A.6}$$

$$\phi_-(\omega) = \frac{1}{\lambda_B} e^{-\omega/\lambda_B} - \frac{\lambda_E^2 - \lambda_H^2}{9\lambda_B^3} \left[1 - \frac{2\omega}{\lambda_B} + \frac{\omega^2}{2\lambda_B^2} \right] e^{-\omega/\lambda_B}, \tag{A.7}$$

$$\begin{aligned}
g_+(\omega) &= -\frac{\lambda_E^2}{6\lambda_B^2} \left\{ (\omega - 2\lambda_B) \text{Ei} \left(-\frac{\omega}{\lambda_B} \right) + \left[(\omega + 2\lambda_B) \left(\ln \frac{\omega}{\lambda_B} + \gamma_E \right) - 2\omega \right] e^{-\omega/\lambda_B} \right\} \\
&+ \frac{\omega^2}{2\lambda_B} \left\{ 1 - \frac{1}{36\lambda_B^2} (\lambda_E^2 - \lambda_H^2) \right\} e^{-\omega/\lambda_B}, \tag{A.8}
\end{aligned}$$

$$g_-^{\text{WW}}(\omega) = \frac{3}{4} \omega e^{-\omega/\lambda_B} \tag{A.9}$$

³All the DAs are given explicitly in Ref. [22], except for g_- , for which we use the model given in Ref. [21].

$$\phi_3(\omega_1, \omega_2) = \frac{\lambda_E^2 - \lambda_H^2}{6\lambda_B^5} \omega_1 \omega_2^2 e^{-(\omega_1 + \omega_2)/\lambda_B}, \quad (\text{A.10})$$

$$\phi_4(\omega_1, \omega_2) = \frac{\lambda_E^2 + \lambda_H^2}{6\lambda_B^4} \omega_2^2 e^{-(\omega_1 + \omega_2)/\lambda_B} \quad (\text{A.11})$$

$$\psi_4(\omega_1, \omega_2) = \frac{\lambda_E^2}{3\lambda_B^4} \omega_1 \omega_2 e^{-(\omega_1 + \omega_2)/\lambda_B}, \quad (\text{A.12})$$

$$\tilde{\psi}_4(\omega_1, \omega_2) = \frac{\lambda_H^2}{3\lambda_B^4} \omega_1 \omega_2 e^{-(\omega_1 + \omega_2)/\lambda_B}, \quad (\text{A.13})$$

where Ei is the exponential integral. These models depend on three independent parameters One is the inverse moment λ_B of the twist-two DA:

$$\lambda_B^{-1} = \int_0^\infty d\omega \frac{\phi_+(\omega)}{\omega}, \quad (\text{A.14})$$

for which we neglect the scale dependence. The adopted values of this and the remaining two parameters λ_E^2 and λ_H^2 are given in Table 3 and their origin is explained in Section 4.3.

B OPE coefficients

In this appendix we present the expressions obtained for the nonvanishing coefficients for the OPE calculation of Eqs. (4.13)-(4.16).

B.1 Contributions of two-particle DAs

The coefficients for the contributions of two-particle DAs to $\mathcal{F}_{\text{OPE}}^{(p)}$ are:

$$\begin{aligned} \mathcal{C}_{\phi_+}^{(p,1)} &= m_B - \frac{m_c}{\bar{\sigma}}, \\ \mathcal{C}_{\Phi_\pm}^{(p,1)} &= -\frac{1}{\bar{\sigma}}, & \mathcal{C}_{\Phi_\pm}^{(p,2)} &= -\frac{m_c(\bar{\sigma}m_B - m_c)}{\bar{\sigma}^2}, \\ \mathcal{C}_{g_+}^{(p,2)} &= \frac{4m_B}{\bar{\sigma}}, & \mathcal{C}_{g_+}^{(p,3)} &= -\frac{8m_c^2(\bar{\sigma}m_B - m_c)}{\bar{\sigma}^3}, \\ \mathcal{C}_{\bar{G}_\pm}^{(p,4)} &= \frac{24m_c^3(\bar{\sigma}m_B - m_c)}{\bar{\sigma}^4}, \end{aligned} \quad (\text{B.1})$$

and to $\mathcal{F}_{\text{OPE}}^{(q)}$ are:

$$\begin{aligned} \mathcal{C}_{\phi_+}^{(q,1)} &= -\frac{\sigma m_B + m_c}{\bar{\sigma}}, \\ \mathcal{C}_{\Phi_\pm}^{(q,1)} &= -\frac{1}{\bar{\sigma}}, & \mathcal{C}_{\Phi_\pm}^{(q,2)} &= \frac{m_c(\sigma m_B + m_c)}{\bar{\sigma}^2}, \\ \mathcal{C}_{g_+}^{(q,2)} &= -\frac{4\sigma m_B}{\bar{\sigma}^2}, & \mathcal{C}_{g_+}^{(q,3)} &= \frac{8m_c^2(\sigma m_B + m_c)}{\bar{\sigma}^3}, \\ \mathcal{C}_{\bar{G}_\pm}^{(q,4)} &= -\frac{24m_c^3(\sigma m_B + m_c)}{\bar{\sigma}^4}, \end{aligned} \quad (\text{B.2})$$

where $\bar{\sigma} \equiv 1 - \sigma$.

B.2 Contributions of three-particle DAs

The coefficients for the contributions of three-particle DAs to $\mathcal{F}_{\text{OPE}}^{(p)}$ are:

$$\begin{aligned}
\mathcal{C}_{\chi_1}^{(p,1)} &= \frac{2(1-u)}{\bar{\sigma}m_B}, \quad \mathcal{C}_{\chi_1}^{(p,2)} = \frac{\bar{\sigma}^2(1-4u)m_B^2 + 3\bar{\sigma}m_Bm_c + 2(1-u)(m_c^2 - q^2)}{\bar{\sigma}m_B}; \\
\mathcal{C}_{\chi_2}^{(p,2)} &= 3(\bar{\sigma}um_B - m_c); \\
\mathcal{C}_{\chi_3}^{(p,2)} &= \frac{m_c}{\bar{\sigma}m_B} + \frac{1}{2} - u, \\
\mathcal{C}_{\chi_3}^{(p,3)} &= \frac{\bar{\sigma}(1-2u)m_B(\bar{\sigma}^2m_B^2 - q^2 - m_c^2) - (\bar{\sigma}^2m_B^2 + q^2)m_c + m_c^3}{\bar{\sigma}m_B}; \\
\mathcal{C}_{\chi_4}^{(p,3)} &= 6m_c(\bar{\sigma}m_B + (1-2u)m_c); \\
\mathcal{C}_{\chi_5}^{(p,2)} &= \frac{1}{2} - \frac{m_c}{\bar{\sigma}m_B}, \quad \mathcal{C}_{\chi_5}^{(p,3)} = \frac{(\bar{\sigma}m_B - m_c)(\bar{\sigma}^2m_B^2 + 2\bar{\sigma}m_Bm_c + m_c^2 - q^2)}{\bar{\sigma}m_B}; \\
\mathcal{C}_{\chi_6}^{(p,3)} &= 6m_c(m_c - \bar{\sigma}m_B); \\
\mathcal{C}_{\chi_7}^{(p,3)} &= -\frac{6m_c^2(1-2u)}{\bar{\sigma}m_B}, \\
\mathcal{C}_{\chi_7}^{(p,4)} &= \frac{6m_c(-\bar{\sigma}^3m_B^3 + (1-2u)(\bar{\sigma}^2m_B^2 + q^2)m_c + \bar{\sigma}m_B(m_c^2 + q^2) - (1-2u)m_c^3)}{\bar{\sigma}m_B}; \\
\mathcal{C}_{\chi_8}^{(p,3)} &= 6m_c, \quad \mathcal{C}_{\chi_8}^{(p,4)} = 18(\bar{\sigma}(1-2u)m_B + m_c)m_c^2; \tag{B.3}
\end{aligned}$$

and to $\mathcal{F}_{\text{OPE}}^{(q)}$ are:

$$\begin{aligned}
\mathcal{C}_{\chi_1}^{(q,1)} &= \frac{2(1-u)}{\bar{\sigma}m_B}, \\
\mathcal{C}_{\chi_1}^{(q,2)} &= \frac{\bar{\sigma}(\bar{\sigma}(1-4u) + 1 + 2u)m_B^2 + 3\bar{\sigma}m_Bm_c + 2(1-u)(m_c^2 - q^2)}{\bar{\sigma}m_B}; \\
\mathcal{C}_{\chi_2}^{(q,2)} &= -3(\sigma um_B + m_c); \\
\mathcal{C}_{\chi_3}^{(q,2)} &= \frac{(\bar{\sigma} - 2)(1-2u)m_B + 2m_c}{2\bar{\sigma}m_B}, \\
\mathcal{C}_{\chi_3}^{(q,3)} &= \frac{1}{\bar{\sigma}m_B} \left[-\bar{\sigma}^2m_B^3\sigma(1-2u) - (\bar{\sigma} - 2)\bar{\sigma}m_B^2m_c - (1-2u)m_B \right. \\
&\quad \left. \times ((1 + \bar{\sigma})m_c^2 - \sigma q^2) + m_c(m_c^2 - q^2) \right]; \\
\mathcal{C}_{\chi_4}^{(q,3)} &= 6m_c(-\sigma m_B + (1-2u)m_c); \\
\mathcal{C}_{\chi_5}^{(q,2)} &= \frac{(\bar{\sigma} - 2)m_B - 2m_c}{2\bar{\sigma}m_B}; \\
\mathcal{C}_{\chi_5}^{(q,3)} &= -\frac{(\sigma m_B + m_c)(\bar{\sigma}^2m_B^2 + 2\bar{\sigma}m_Bm_c + m_c^2 - q^2)}{\bar{\sigma}m_B};
\end{aligned}$$

$$\begin{aligned}
\mathcal{C}_{\chi_6}^{(q,3)} &= 6m_c(\sigma m_B + m_c); \\
\mathcal{C}_{\chi_7}^{(q,3)} &= \frac{6m_c(m_B - (1 - 2u)m_c)}{\bar{\sigma}m_B}, \\
\mathcal{C}_{\chi_7}^{(q,4)} &= \frac{6m_c}{\bar{\sigma}m_B} \left[\sigma\bar{\sigma}^2 m_B^3 + \bar{\sigma}(\bar{\sigma} - 2)(1 - 2u)m_B^2 m_c + (1 + \bar{\sigma})m_B m_c^2 \right. \\
&\quad \left. - \sigma m_B q^2 - (1 - 2u)m_c(m_c^2 - q^2) \right]; \\
\mathcal{C}_{\chi_8}^{(q,3)} &= 6m_c, \quad \mathcal{C}_{\chi_8}^{(q,4)} = 18m_c^2(-\sigma(1 - 2u)m_B + m_c).
\end{aligned} \tag{B.4}$$

Here the parameter u is a function of σ , ω_1 , and ω_2 :

$$u = \frac{\sigma m_B - \omega_1}{\omega_2}, \tag{B.5}$$

which induces a ω_1, ω_2 dependence in Eq. (4.16) for the coefficients at the three-particle DAs.

References

- [1] N. Gubernari, A. Khodjamirian, R. Mandal and T. Mannel, JHEP **05** (2022), 029 [arXiv:2203.08493 [hep-ph]].
- [2] P. Colangelo, G. Nardulli, A. A. Ovchinnikov and N. Paver, Phys. Lett. B **269** (1991), 201-207.
- [3] P. Colangelo, F. De Fazio and N. Paver, Phys. Rev. D **58** (1998), 116005 [arXiv:hep-ph/9804377 [hep-ph]].
- [4] R. L. Workman *et al.* [Particle Data Group], PTEP **2022** (2022), 083C01
- [5] M. L. Du, F. K. Guo, C. Hanhart, B. Kubis and U. G. Meißner, Phys. Rev. Lett. **126** (2021) no.19, 192001 [arXiv:2012.04599 [hep-ph]].
- [6] M. L. Du, M. Albaladejo, P. Fernández-Soler, F. K. Guo, C. Hanhart, U. G. Meißner, J. Nieves and D. L. Yao, Phys. Rev. D **98** (2018) no.9, 094018 [arXiv:1712.07957 [hep-ph]].
- [7] L. Gayer *et al.* [Hadron Spectrum], JHEP **07** (2021), 123 [arXiv:2102.04973 [hep-lat]].
- [8] M. Ablikim *et al.* [BESIII], Phys. Rev. D **97** (2018) no.5, 051103 [arXiv:1711.08293 [hep-ex]].
- [9] R. Aaij *et al.* [LHCb], Phys. Rev. D **94** (2016) no.7, 072001 [arXiv:1608.01289 [hep-ex]].
- [10] M. A. Shifman, A. I. Vainshtein and V. I. Zakharov, Nucl. Phys. B **147** (1979), 385-447
- [11] P. Gelhausen, A. Khodjamirian, A. A. Pivovarov and D. Rosenthal, Eur. Phys. J. C **74** (2014) no.8, 2979 [arXiv:1404.5891 [hep-ph]].
- [12] M. Jamin and M. Munz, Z. Phys. C **60** (1993), 569-578 [arXiv:hep-ph/9208201 [hep-ph]].

- [13] P. Gelhausen, A. Khodjamirian, A. A. Pivovarov and D. Rosenthal, Phys. Rev. D **88** (2013), 014015 [erratum: Phys. Rev. D **89** (2014), 099901; erratum: Phys. Rev. D **91** (2015), 099901] [arXiv:1305.5432 [hep-ph]].
- [14] A. Khodjamirian, B. Melić, Y. M. Wang and Y. B. Wei, JHEP **03** (2021), 016 [arXiv:2011.11275 [hep-ph]].
- [15] Y. Aoki *et al.* [Flavour Lattice Averaging Group (FLAG)], Eur. Phys. J. C **82** (2022) no.10, 869 [arXiv:2111.09849 [hep-lat]].
- [16] B. L. Ioffe, Phys. Atom. Nucl. **66** (2003), 30-43 [arXiv:hep-ph/0207191 [hep-ph]].
- [17] P. Colangelo, F. De Fazio and A. Ozpineci, Phys. Rev. D **72** (2005), 074004 [arXiv:hep-ph/0505195 [hep-ph]].
- [18] A. Khodjamirian, T. Mannel and N. Offen, Phys. Rev. D **75** (2007), 054013 [arXiv:hep-ph/0611193 [hep-ph]].
- [19] I. I. Balitsky and V. M. Braun, Nucl. Phys. B **311** (1989), 541-584
- [20] S. Faller, A. Khodjamirian, C. Klein and T. Mannel, Eur. Phys. J. C **60** (2009), 603-615 [arXiv:0809.0222 [hep-ph]].
- [21] N. Gubernari, A. Kokulu and D. van Dyk, JHEP **01** (2019), 150 [arXiv:1811.00983 [hep-ph]].
- [22] V. M. Braun, Y. Ji and A. N. Manashov, JHEP **05** (2017), 022 [arXiv:1703.02446 [hep-ph]].
- [23] S. Descotes-Genon, A. Khodjamirian and J. Virto, JHEP **12** (2019), 083 [arXiv:1908.02267 [hep-ph]].
- [24] V. M. Braun, D. Y. Ivanov and G. P. Korchemsky, Phys. Rev. D **69** (2004), 034014 [arXiv:hep-ph/0309330 [hep-ph]].
- [25] A. Khodjamirian, R. Mandal and T. Mannel, JHEP **10** (2020), 043 [arXiv:2008.03935 [hep-ph]].
- [26] M. Rahimi and M. Wald, Phys. Rev. D **104** (2021) no.1, 016027 [arXiv:2012.12165 [hep-ph]].
- [27] T. Nishikawa and K. Tanaka, Nucl. Phys. B **879** (2014), 110-142 [arXiv:1109.6786 [hep-ph]].
- [28] A. G. Grozin and M. Neubert, Phys. Rev. D **55** (1997), 272-290 [arXiv:hep-ph/9607366 [hep-ph]].
- [29] T. Feldmann, P. Lüghausen and N. Seitz, JHEP **08** (2023), 075 doi:10.1007/JHEP08(2023)075 [arXiv:2306.14686 [hep-ph]].
- [30] N. Gubernari, D. van Dyk and J. Virto, JHEP **02** (2021), 088 [arXiv:2011.09813 [hep-ph]].
- [31] W. Detmold, C. Lehner and S. Meinel, Phys. Rev. D **92** (2015) no.3, 034503 [arXiv:1503.01421 [hep-lat]].

- [32] F. U. Bernlochner and Z. Ligeti, Phys. Rev. D **95** (2017) no.1, 014022 [arXiv:1606.09300 [hep-ph]].
- [33] F. U. Bernlochner, Z. Ligeti and D. J. Robinson, Phys. Rev. D **97** (2018) no.7, 075011 doi:10.1103/PhysRevD.97.075011 [arXiv:1711.03110 [hep-ph]].
- [34] Y. B. Zuo, H. Y. Jin, J. Y. Tian, J. Yi, H. Y. Gong and T. T. Pan, Chin. Phys. C **47** (2023) no.10, 103104 doi:10.1088/1674-1137/ace821 [arXiv:2307.08271 [hep-ph]].